Photochemistry

International Edition: DOI: 10.1002/anie.201606775
German Edition: DOI: 10.1002/ange.201606775

Tailoring Transition-Metal Hydroxides and Oxides by Photon-Induced Reactions

*Kai-Yang Niu[+], Liang Fang[+], Rong Ye[+], Dennis Nordlund, Marca M. Doeff, Feng Lin, and Haimei Zheng**

Abstract: *Controlled synthesis of transition-metal hydroxides and oxides with earth-abundant elements have attracted significant interest because of their wide applications, for example as battery electrode materials or electrocatalysts for fuel generation. Here, we report the tuning of the structure of transition-metal hydroxides and oxides by controlling chemical reactions using an unfocused laser to irradiate the precursor solution. A Nd:YAG laser with wavelengths of 532 nm or 1064 nm was used. The Ni^{2+}, Mn^{2+}, and Co^{2+} ion-containing aqueous solution undergoes photo-induced reactions and produces hollow metal-oxide nanospheres ($Ni_{0.18}Mn_{0.45}Co_{0.37}O_x$) or core–shell metal hydroxide nanoflowers ($[Ni_{0.15}Mn_{0.15}Co_{0.7}(OH)_2](NO_3)_{0.2}\cdot H_2O$), depending on the laser wavelengths. We propose two reaction pathways, either by photo-induced redox reaction or hydrolysis reaction, which are responsible for the formation of distinct nanostructures. The study of photon-induced materials growth shines light on the rational design of complex nanostructures with advanced functionalities.*

Laser has been used for the study of photon-matter interactions for decades since its invention in 1960s,[1] and a variety of synthetic methodologies, such as laser pyrolysis,[2] pulsed laser deposition,[3] have been developed for the production of functional composite materials. In recent years, intensive studies have focused on nanomaterials syntheses using laser ablation/irradiation in solution phases,[4] and two liquid-based laser techniques, that is, pulsed laser ablation of a solid target in liquids (PLAL)[5] and pulsed laser irradiation of colloidal nanoparticles in liquids (PLICN),[6] have been widely adopted. From these techniques, diverse complex nanoparticles and nanostructures have been fabricated, and deeper understanding of the materials formation from the laser–matter interactions has also been addressed.[6c] In contrast to the "top–down" synthesis of the laser ablation of bulk solids in liquids, a "bottom–up" method, that is, pulsed laser irradiation of a precursor solution, where nucleation and growth of materials are expected from the laser-mediated chemical reactions, is also a promising liquid-based laser protocol for complex materials design.[7]

Using laser photons to initiate and control the chemical reactions to yield certain products has always been a central mission in laser chemistry, and exceptional achievements have been accomplished in laser-controlled reactions in molecular science. It is also expected that laser photons can be used to control chemical reactions in solutions for the design of diverse complex materials,[7a–c] although understanding is limited. So far, laser irradiation has been successfully applied to several precursor solutions, mostly those containing noble metal ions,[7b] from which noble metal nanoparticles or alloys, such as Au-Ag,[8] Rh-Pd-Pt,[9] have been obtained. Despite all these achievements, the reaction mechanisms in the laser solution chemistry for materials growth are still far from fully understood. Herein, we aim to unravel the different pathways of laser-mediated chemical reactions in aqueous precursor solutions, and to demonstrate the flexibility and diversity of laser solution chemistry for tailoring various complex nanostructures. An aqueous precursor solution containing $Ni(NO_3)_2$, $Mn(NO_3)_2$ and $Co(NO_3)_2$ was selected as a model system, and an unfocused nanosecond pulsed laser (9 mm in diameter) with pulse energy of 750 mJ at 1064 nm and 350 mJ at 532 nm was used for the laser irradiation experiments. Both the powder products and precursor solutions after laser irradiation were collected for examination.

[*] Dr. K.-Y. Niu,[+] Prof. Dr. L. Fang,[+] Dr. H. Zheng
Materials Sciences Division
Lawrence Berkeley National Laboratory
1 Cyclotron Road, Berkeley, California 94720 (USA)
E-mail: hmzheng@lbl.gov
Prof. Dr. L. Fang[+]
State Key Laboratory of Mechanical Transmission
College of Physics, Chongqing University
Chongqing 400044 (China)
R. Ye[+]
Department of Chemistry, University of California
Berkeley, CA 94720 (USA)
Dr. D. Nordlund
Stanford Synchrotron Radiation Lightsource
SLAC National Accelerator Laboratory
Menlo Park, California 94025 (USA)
Dr. M. M. Doeff, Prof. Dr. F. Lin
Energy Storage and Distributed Resources Division
Lawrence Berkeley National Laboratory
1 Cyclotron Road, Berkeley, California 94720 (USA)
Prof. Dr. F. Lin
Department of Chemistry, Virginia Tech
Blacksburg, VA 24061 (USA)
Dr. H. Zheng
Department of Materials Science and Engineering
University of California
Berkeley, CA 94720 (USA)
[+] These authors contributed equally to this work.
Supporting information and the ORCID identification number(s) for the author(s) of this article can be found under http://dx.doi.org/10.1002/anie.201606775.

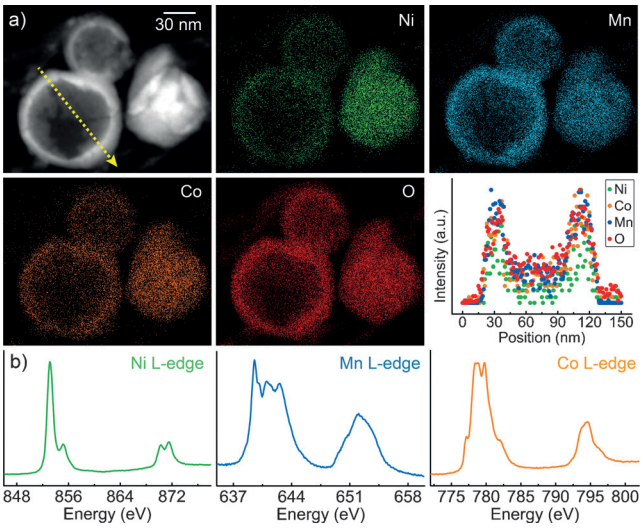

Figure 1. Ni-Mn-Co oxide formed using 532 nm laser light. a) Scanning TEM (STEM) image and EDS mapping of the $Ni_{0.18}Mn_{0.45}Co_{0.37}O_x$ nanospheres (two particles on the left side are hollow) produced by irradiation with 532 nm laser light of an aqueous solution with mixed nickel nitrate, manganese nitrate, and cobalt nitrate, where the molar ratio of Ni:Mn:Co is 0.25:0.25:0.5. The line-scan profile over a hollow sphere shown in the STEM image indicates the anisotropic distribution of Ni, Co, Mn, and O in the sphere. b) Ni L-edge, Mn L-edge, and Co L-edge XAS/TEY spectra of the $Ni_{0.18}Mn_{0.45}Co_{0.37}O_x$ compounds.

Figure 1 shows the morphology, composition and metal valences of the product when the 532 nm laser was applied to the precursor solution. The product contains mostly hollow nanospheres with homogeneous elemental distribution of Ni, Mn, Co and O (Figure 1 a). High-resolution TEM images (see Figure S1 in the Supporting Information) show that the structure of the as-produced particles is similar to cobalt manganese oxide (JCPDS number 18-0409), which is a tetragonal spinel structure intermediate between $MnCo_2O_4$ (cubic) and Mn_3O_4 (tetragonal). Soft X-ray absorption spectroscopy (XAS) was used to determine the valence states of metal ions in the as-prepared powder. The fine structures in the XAS spectra (Figure 1 b) indicate that the nickel has a oxidation state of 2+, cobalt also stays mainly as 2+, and manganese has a mixed valence states of 2+/3+/4+.[10] Based on the EDS analysis, we formulate this compound as $Ni_{0.18}Mn_{0.45}Co_{0.37}O_x$.

Laser irradiation of solutions can induce electronic and/or vibrational excitation of reagent molecules/ions,[1e,11] which can trigger certain chemical reactions and lead to the nucleation and growth of certain materials.[7a–c] Under 532 nm laser irradiation, water molecules can be ionized due to multi-photon excitation.[8] Thus, various reactive species,[12] including solvated electrons (e_{aq}^-), hydrogen radicals (H·), hydroxy radicals (OH·), and H_3O^+, could be generated within 10^{-12} s, then they react with each other and/or the surrounding molecules in a timescale of 10^{-12}–10^{-6} s.[13] The free metal ions (M^{x+}) in the aqueous solution could be reduced into pure metal (M^0) instantaneously by the e_{aq}^- and H· in a nanosecond laser pulse. This explains the particle growth when use a short-wavelength laser to irradiate the aqueous solution of noble-metal salts, where pure metal nanoparticles were produced.[8,14] In this study, the as-grown transition-metal nanoparticles are prone to fast oxidation in the aqueous solution because of the oxidative nature of the laser-induced OH· radicals. Once a thin oxide is formed, the Kirkendall effect,[15] or selective laser irradiation[16] of the oxidized metal nanoparticles leads to the formation of hollow metal-oxide nanoparticles (Figure 1 a and Figure S1).

Besides the electronic ionization of water molecules by the 532 nm laser, we discovered another major reaction pathway for accessing distinct complex nanostructures when 1064 nm laser irradiation in the aqueous solution was performed.

Figure 2 provides the structure information of the as-synthesized composite produced by the 1064 nm laser irradiation of the aqueous precursor solution containing Ni^{2+}, Mn^{2+} and Co^{2+}. The XRD pattern reveals that the material is isostructural with the rhombohedral α-nickel hydroxide (JCPDS 380715, line markers in Figure 2 a), where the *d* spacing of the (003) peak is about 7.0 Å. The thermogravimetric analysis (TGA, Figure 2 b) shows a 26% weight loss of the material below about 280 °C, corresponding to an 8% loss of absorbed and structurally bonded water and an 18% loss due to the evolution of H_2O and NO_2 upon heating of a hydroxide material. In the Fourier transform infrared spectra (Figure 2 c), we can identify the absorption of OH stretching (3410 cm^{-1}), H_2O (1640 cm^{-1}), and $NO_3^-{\cdot}H_2O$ (1318 cm^{-1} and 1413 cm^{-1}) in the material.[17] The enlarged fingerprint region (below 1100 cm^{-1}, Figure 2 d) shows the M^{x+}-O stretching and M^{x+}-O-H bending modes,[18] which can be specifically assigned to OO^- stretching (1046 cm^{-1} and 985 cm^{-1}), sym-MnO_2 (822 cm^{-1}), Ni/Co-O-H stretching (794 cm^{-1}), Ni/Co-O-H bending (513 cm^{-1}), weak Mn-O vibrations in MnO_2 (700 cm^{-1}, 541 cm^{-1} and 474 cm^{-1}), Mn-O vibrations in MnOOH (640 cm^{-1}, 583 cm^{-1} and 448 cm^{-1}) Mn-O-H stretching (700 cm^{-1}), and Mn-O-H bending (425 cm^{-1}). Based on the structural and elemental analyses,

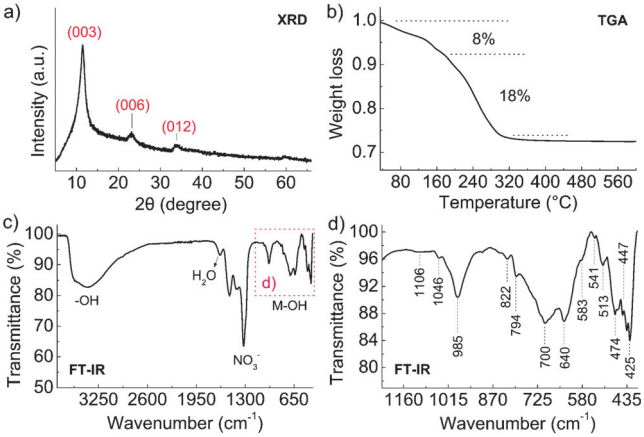

Figure 2. Identification of Ni-Mn-Co-OH formed using 1064 nm laser. a) XRD pattern, b) TGA curve, c) and d) FT-IR spectra of the as-prepared powder of Ni-Mn-Co-OH composite synthesized by irradiating the aqueous precursor solution containing Ni^{2+}, Mn^{2+} and Co^{2+} with Ni:Mn:Co molar ratio of 0.25:0.25:0.5 with 1064 nm laser light.

we determined that the as-synthesized materials by a 1064 nm laser are 3d metal complex hydroxides, formulated as $[Ni_{0.15}Mn_{0.15}Co_{0.7}(OH)_2](NO_3)_{0.2}\cdot H_2O$ (simplified as Ni-Mn-Co-OH), where the positively charged layered metal ion slabs are balanced by the hydroxyl groups (OH), nitrate ions (NO_3^-) and water molecules (H_2O) located likely between the layers.

Figure 3 displays the chemical and structural information of the Ni-Mn-Co-OH. The TEM image (Figure 3a) shows that the particles of the as-prepared nanocomposite have a snowflake-like structure with diameters of 60 nm and thicknesses of 20 nm. Slight compositional segregation, where Ni and Co ions are rich in the center and Mn ions are rich at the edge of the particle, was identified from the EDS mapping (see Figure S2). The XAS spectra (red lines in Figure 3c) indicate that the valence states of the Ni, Mn, and Co ions mainly stay as 2+, 2+/3+, and 2+, respectively.

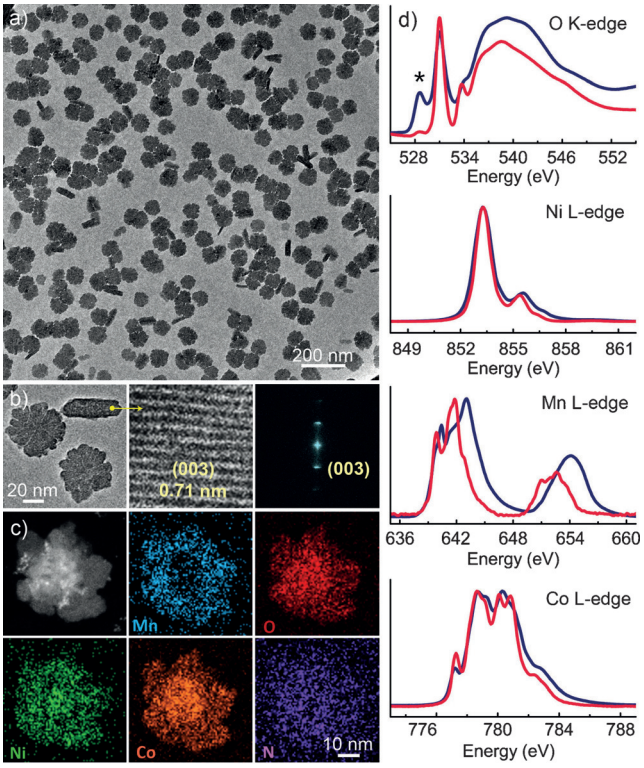

Figure 3. Morphology and structure of Ni-Mn-Co-OH formed using 1064 nm laser. a) TEM image of Ni-Mn-Co-OH composite synthesized by 1064 nm laser irradiation of an aqueous solution with Ni:Mn:Co molar ratio of 0.25:0.25:0.5. b) TEM images with the corresponding FFT pattern, and c) EDS mapping of the Li-Ni-Mn-Co-OH nanoflakes produced by 1064 nm laser irradiation with Li:Ni:Mn:Co molar ratio of 1:0.25:0.25:0.5 in the solution. d) O K-edge, Ni L-edge, Mn L-edge, and Co L-edge XAS/TEY spectra of the as-grown Ni-Mn-Co-OH (red lines) and Li-Ni-Mn-Co-OH (blue lines) nanoflakes. The asterisk indicates the 3d metal-derived states of higher valency Mn ions.

We then add lithium nitrate into the laser-chemical synthesis, considering that Li ions may be inserted in the crystal lattice of the nanoflakes, which gives us chances to further tune structure of the material via one-step laser irradiation. As a result, similar snowflake structure was formed by adding Li^+ (Figure 3b), and the high-resolution TEM image shows that the nanoflake has a layered structure with a layer lattice spacing of 0.71 nm (corresponding to the (003) peak on the XRD pattern in Figure 2a). We also found more severe compositional segregation in the particle (Figure 3c) compared to the one without Li^+, which results in a core–shell structure with a Ni/Co-rich core and a Mn-containing shell. Concomitantly, the metal ions were promoted to their higher valence states (Figure 3d), especially for Mn ions whose valency has increased from 2+/3+ to 4+. Consequently, an increased intensity of the pre-edge of O K-edge (ca. 529 eV, marked with an asterisk) was detected, which is uniquely associated with the 3d metal-derived states (Mn3d-O2p) of higher valency Mn ions,[19] similar to that of MnO_2.[19b]

To further understand the laser-induced reaction mechanisms, we investigated the chemical evolution occurring in the solutions as they were exposed to laser irradiation at different times. Upon laser irradiation, the original bright-red solution darkened, and precipitates formed in the solution after 40 min laser irradiation (Figure S3a). The FT-IR spectra of the solutions in Figure 4a display the major vibrational absorptions of OH, H_2O, and NO_3^- from the aqueous nitrate

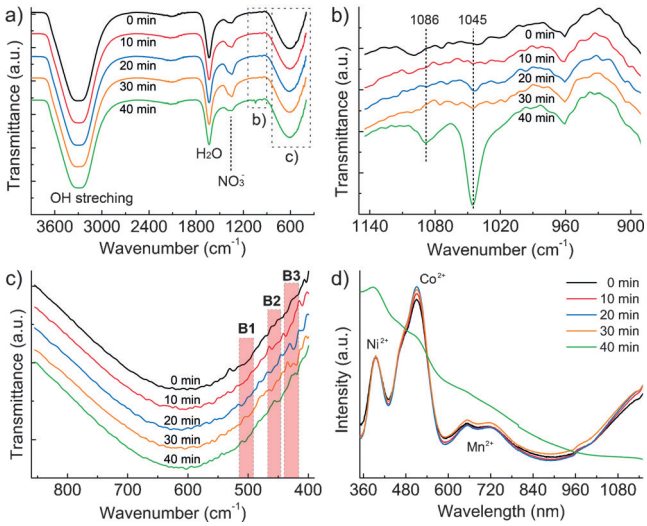

Figure 4. FT-IR and UV/Vis spectroscopy of Ni-Mn-Co-OH formed using 1064 nm laser light. a–c) FT-IR spectra of the aqueous solution containing Ni^{2+}, Mn^{2+}, and Co^{2+} ions upon 1064 nm laser irradiation at different times. Spectra (b) and (c) are the enlarged FT-IR spectra as framed in the full spectrum in (a). Note that the spectra are original and have not been smoothed. d) UV/Vis absorption spectra of the laser-irradiated solutions corresponding to (a).

solution, as well as weak absorption bands related to the precipitates. In Figure 4b, it can be clearly seen that two obvious absorption bands appear around 1086 cm^{-1} and 1045 cm^{-1}. These two bands are too high for the OO^- stretching modes of peroxide moieties (such as MOOH or MOOM), which are usually in the 920–740 cm^{-1} region.[20] However, they are quite similar to the OO^- stretching frequencies where a superoxo bridge forms between two metal centers, such as the as-reported superoxide moiety

(1160–1015 cm^{-1}) in CoO-MgO solid solutions and the inorganic dibridged superoxo complexes of Co^{III} centers (1068 cm^{-1}) in μ-amido-μ-hyperoxo bis[tetraamminecobalt-(III)].[21] It is likely that, under these conditions, the superoxo-bridge configuration of complex metal hydroxides (such as NiOOMn or CoOOMn) forms as a bonding pathway upon laser irradiation of the aqueous nitrate solutions.

In addition, several -OH bending absorption bands in the fingerprint region, shown as B1 (510–505 cm^{-1}), B2 (463–450 cm^{-1}) and B3 (430–420 cm^{-1}) in Figure 4c (also see Figure S3b), are also identified, indicating the formation of $Ni/Co(OH)_2$, OCo(OH), and $Mn(OH)_2$ clusters[15] in the solutions upon laser irradiation. By examining the UV/Vis absorption of the solutions (Figure 4d) in the same time frame, it can be seen that the absorption bands of metal ions in the nitrates or molecular M-O(O)H clusters are dominant in the solutions in the first 30 min laser irradiation, then a distinct absorption feature of the hydroxide precipitates becomes evident after 40 min, indicative of the drastic growth of particles from the supersaturation of accumulative M-O(O)H clusters in the solution.

Based on the above analyses, we summarize two reaction pathways for tailoring different materials when use laser light of different wavelengths (that is, 532 nm or 1064 nm) to irradiate the precursor solution (Scheme 1). For the 532 nm laser irradiation (Path **I**), due to multi-photon ionization

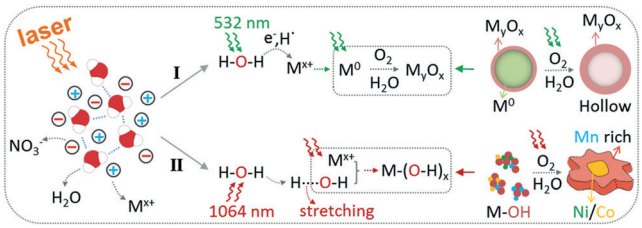

Scheme 1. Summary of the two possible reaction pathways for tailoring distinct complex nanostructures by irradiating aqueous 3d metal nitrates solutions with laser light, where M stands for Ni, Co, and Mn.

excitation of the liquid water molecules, reductive species such as solvated electrons (e_{aq}^-) and hydrogen radicals (H·) could be released in the solution,[6] and reduce the free metal ions (M^{x+}) into pure metal atoms (M^0). Prolonged laser irradiation causes accumulation of metal atoms which leads to the nucleation/growth of metal nanoparticles. Because of the high reactivity of 3d metals, the as-formed metal nanoparticles are prone to surface oxidation, and hollow transition-metal-oxide nanoparticles could form via laser-heating-promoted Kirkendall effect on the oxidized metal nanoparticles.[10]

For the 1064 nm laser irradiation, since liquid water molecules have combined vibrational absorptions in the wavelength range of 500–1200 nm, the laser photons can stretch H-O-H bonds through intense vibrational excitations, where the ionization of H_2O molecules seems weak. Meanwhile, we found that the existence of Ni ions can highly promote the reaction rate. The three-spin-allowed electronic transitions of d^8 Ni^{2+}, that is, $^3A_{2g}(F)\rightarrow{}^3T_{1g}(P)$, $^3A_{2g}(F)\rightarrow{}^3T_{1g}(F)$ and $^3A_{2g}(F)\rightarrow{}^3T_{2g}(F)$ with absorption bands around 365 nm, 650 nm, and 1080 nm,[22] respectively, could be excited by the laser, which may transfer more energy to the vibrational states of water molecules and make them much stretched. Because of the enhanced reactivity of stretched water,[23] the complex hydrolysis reactions between the activated hydroxy radicals and the positively charged metal ions can be initiated, resulting in the growth of complex hydroxides. The major chemical reactions could be written as shown in Equations (1)–(8).

$$Ni^{2+} + 2\,H_2O \xrightarrow{nh\nu} Ni(OH)_2 + H^+ \quad (1)$$

$$Co^{2+} + 2\,H_2O \xrightarrow{nh\nu} Co(OH)_2 + H^+ \quad (2)$$

$$Mn^{2+} + 2\,H_2O \xrightarrow{nh\nu} Mn(OH)_2 + H^+ \quad (3)$$

$$2Mn^{2+} + O_2 + 4\,H_2O \rightarrow 4\,Mn^{3+} + 4\,OH^- \quad (4)$$

$$Mn^{3+} + 3\,OH^- \rightarrow Mn(OH)_3 \quad (5)$$

$$4\,Mn(OH)_2 + O_2 \rightarrow 4\,MnOOH + 2\,H_2O \quad (6)$$

$$4\,Co(OH)_2 + O_2 \rightarrow 4\,CoOOH + 2\,H_2O \quad (7)$$

$$2\,Mn(OH)_2 + O_2 \rightarrow 2\,MnO_2 + 2\,H_2O \quad (8)$$

In summary, we have tailored the structure of transition-metal hydroxides and oxides by controlling chemical reactions using an unfocused laser beam to irradiate the precursor solution containing multiple 3d metal ions. Two distinct reaction pathways were unraveled when selecting different laser wavelengths (532 nm or 1064 nm). The 532 nm laser can induce ionization excitation of water molecules and release reducing species such as solvated electrons (e_{aq}^-) and hydrogen radicals (H·) in the solution, which then reduce the metal ions into metal nanoparticles, and further laser heating then leads to hollow metal-oxide nanoparticles. When a 1064 nm laser is used, vibrational excitation of water molecules become the dominant events, the OH groups of water molecules are considerably stretched, which facilitates the hydrolysis reaction of metal ions and results in the growth of complex hydroxide nanostructures. It was also discovered that the structure and metal valences of the complex hydroxides can be easily tuned by either changing the ratio of metal components or introducing additional ions (such as Li^+) in the precursor solutions. Future work using the laser solution chemistry will aim at design of more functional nanocomposites and including correlation of the described structural properties with advanced materials performances such as the photo/electrocatalysis.

Acknowledgements

We used Tecnai and TitanX microscopes for structural analysis at National Center for Electron Microscopy of Lawrence Berkeley National Laboratory (LBNL), which is supported by the U.S. Department of Energy Office of Basic Energy Sciences under contract number DE-AC02-05CH11231. The synchrotron X-ray portions of this research

were carried out at the Stanford Synchrotron Radiation Lightsource (Beam Lines 10-1 and 8-2), a Directorate of SLAC National Accelerator Laboratory and an Office of Science User Facility operated for the U.S. Department of Energy Office of Science by Stanford University. K.N. thanks Dr. Xin Liu for the help on the UV/Vis absorption spectra. L.F. acknowledges the support of National Natural Science Foundation of China (NSFC) under numbers 11544010 and 11547305. F.L. acknowledges the support from Virginia Tech. F.L. and D.N. thank Dr. Jun-Sik Lee and Glen Kerr for the help at SSRL Beam Line 8-2. H.Z. acknowledges the SinBeRise program of BEARS at University of California, Berkeley for travel support. She thanks the support of DOE Office of Science Early Career Research Program.

Keywords: nanostructures · photochemistry · reaction pathways · transition-metal hydroxides · vibrational excitation

How to cite: *Angew. Chem. Int. Ed.* **2016**, *55*, 14272–14276
Angew. Chem. **2016**, *128*, 14484–14488

[1] a) R. M. Osgood, T. F. Deutsch, *Science* **1985**, *227*, 709–714; b) G. B. Blanchet, C. R. Fincher, C. L. Jackson, S. I. Shah, K. H. Gardner, *Science* **1993**, *262*, 719–721; c) A. L. Robinson, *Science* **1976**, *193*, 1230–1276; d) T. H. Maiman, *Nature* **1960**, *187*, 493–494; e) D. L. Rousseau, *J. Chem. Educ.* **1966**, *43*, 566–570.

[2] F. Huisken, G. Ledoux, O. Guillois, C. Reynaud, *Adv. Mater.* **2002**, *14*, 1861–1865.

[3] P. R. Willmott, J. R. Huber, *Rev. Mod. Phys.* **2000**, *72*, 315–328.

[4] S. Barcikowski, F. Mafuné, *J. Phys. Chem. C* **2011**, *115*, 4985–4985.

[5] a) H. Zeng, X.-W. Du, S. C. Singh, S. A. Kulinich, S. Yang, J. He, W. Cai, *Adv. Funct. Mater.* **2012**, *22*, 1333–1353; b) G. W. Yang, *Prog. Mater. Sci.* **2007**, *52*, 648–698; c) K.-Y. Niu, J. Yang, S. Kulinich, J. Sun, H. Li, X. Du, *J. Am. Chem. Soc.* **2010**, *132*, 9814–9819.

[6] a) H. Wang, A. Pyatenko, K. Kawaguchi, X. Li, Z. Swiatkowska-Warkocka, N. Koshizaki, *Angew. Chem. Int. Ed.* **2010**, *49*, 6361–6364; *Angew. Chem.* **2010**, *122*, 6505–6508; b) K.-Y. Niu, H.-M. Zheng, Z.-Q. Li, J. Yang, J. Sun, X.-W. Du, *Angew. Chem. Int. Ed.* **2011**, *50*, 4099–4102; *Angew. Chem.* **2011**, *123*, 4185–4188; c) J. Yang, T. Ling, W.-T. Wu, H. Liu, M.-R. Gao, C. Ling, L. Li, X.-W. Du, *Nat. Commun.* **2013**, *4*, 1695.

[7] a) H. Liu, P. Jin, Y.-M. Xue, C. Dong, X. Li, C.-C. Tang, X.-W. Du, *Angew. Chem. Int. Ed.* **2015**, *54*, 7051–7054; *Angew. Chem.* **2015**, *127*, 7157–7160; b) M. R. Langille, M. L. Personick, C. A. Mirkin, *Angew. Chem. Int. Ed.* **2013**, *52*, 13910–13940; *Angew. Chem.* **2013**, *125*, 14158–14189; c) K.-Y. Niu, F. Lin, S. Jung, L. Fang, D. Nordlund, C. C. L. McCrory, T.-C. Weng, P. Ercius, M. M. Doeff, H. Zheng, *Nano Lett.* **2015**, *15*, 2498–2503; d) K.-Y. Niu, F. Lin, L. Fang, D. Nordlund, R. Tao, T.-C. Weng, M. M. Doeff, H. Zheng, *Chem. Mater.* **2015**, *27*, 1583–1589.

[8] R. Kuladeep, L. Jyothi, K. S. Alee, K. L. N. Deepak, D. N. Rao, *Opt. Mater. Express* **2012**, *2*, 161–172.

[9] M. S. Islam Sarker, T. Nakamura, S. Sato, *J. Mater. Res.* **2014**, *29*, 856–864.

[10] a) F. Lin, I. M. Markus, D. Nordlund, T.-C. Weng, M. D. Asta, H. L. Xin, M. M. Doeff, *Nat. Commun.* **2014**, *5*, 3529; b) K. Pecher, D. McCubbery, E. Kneedler, J. Rothe, J. Bargar, G. Meigs, L. Cox, K. Nealson, B. Tonner, *Geochim. Cosmochim. Acta* **2003**, *67*, 1089–1098.

[11] K. Kleinermanns, J. Wolfrum, *Angew. Chem. Int. Ed. Engl.* **1987**, *26*, 38–58; *Angew. Chem.* **1987**, *99*, 38–58.

[12] C. L. Thomsen, D. Madsen, S. R. Keiding, J. Tho/gersen, O. Christiansen, *J. Chem. Phys.* **1999**, *110*, 3453–3462.

[13] S. Le Caër, *Water* **2011**, *3*, 235–253.

[14] J. P. Abid, A. W. Wark, P. F. Brevet, H. H. Girault, *Chem. Commun.* **2002**, 792–793.

[15] a) K.-Y. Niu, J. Park, H. Zheng, A. P. Alivisatos, *Nano Lett.* **2013**, *13*, 5715–5719; b) W. Wang, M. Dahl, Y. Yin, *Chem. Mater.* **2013**, *25*, 1179–1189; c) A. Cabot, M. Ibáñez, P. Guardia, A. P. Alivisatos, *J. Am. Chem. Soc.* **2009**, *131*, 11326–11328.

[16] K. Y. Niu, J. Yang, S. A. Kulinich, J. Sun, X. W. Du, *Langmuir* **2010**, *26*, 16652–16657.

[17] D. J. Goebbert, E. Garand, T. Wende, R. Bergmann, G. Meijer, K. R. Asmis, D. M. Neumark, *J. Phys. Chem. A* **2009**, *113*, 7584–7592.

[18] a) R. Yang, Z. Wang, L. Dai, L. Chen, *Mater. Chem. Phys.* **2005**, *93*, 149–153; b) X. Wang, L. Andrews, *J. Phys. Chem. A* **2006**, *110*, 10035–10045.

[19] a) B. Gilbert, B. H. Frazer, A. Belz, P. G. Conrad, K. H. Nealson, D. Haskel, J. C. Lang, G. Srajer, G. De Stasio, *J. Phys. Chem. A* **2003**, *107*, 2839–2847; b) F. M. F. de Groot, M. Grioni, J. C. Fuggle, J. Ghijsen, G. A. Sawatzky, H. Petersen, *Phys. Rev. B* **1989**, *40*, 5715–5723.

[20] K. Nakamoto, *Infrared and Raman spectra of inorganic and coordination compounds*, Wiley Online Library, New York, **1986**.

[21] T. Shibahara, M. Mori, *Bull. Chem. Soc. Jpn.* **1978**, *51*, 1374–1379.

[22] S. L. Reddy, G. S. Reddy, T. Endo, *Electronic (absorption) spectra of 3d transition-metal complexes*, INTECH Open Access Publisher, **2012**.

[23] G. C. Schatz, *Science* **2000**, *290*, 950–951.

Received: July 12, 2016
Revised: September 7, 2016
Published online: October 18, 2016

